Korean J. Chem. Eng., **28**(12), 2329-2335 (2011)
DOI: 10.1007/s11814-011-0115-4

Green synthesis of gold nanostructures using pear extract as effective reducing and coordinating agent

Gajanan Ghodake and Dae Sung Lee†

Department of Environmental Engineering, Kyungpook National University, 80 Daehak-ro, Buk-gu, Daegu 702-701, Korea
(*Received 20 February 2011 • accepted 26 April 2011*)

Abstract–Biosynthesis of gold nanoparticles and nanoplates (GNPs) was accomplished using aqueous fractions of pear extract as a safe, reducing, particle-stabilizing, and shape-directing agent. The maximum yields of spherical gold nanoparticles having the average sizes of 40, 20, and 10 nm were achieved at 30, 60, and 90 °C, respectively, at a pear extract concentration of 45% (v/v). The maximum yield of gold nanoplates was obtained with sizes ranging from 20 to 400 nm, particularly at reaction temperatures of 30, 60, and 90 °C, at a pear extract concentration of 5% (v/v). The surface chemistry analysis of the GNPs suggests that the sugars and peptides or proteins as key biomolecules of the pear extract play a crucial role in the reduction of Au(III), subsequently resulting in healthy capping. Therefore, this environmentally friendly synthesis method of GNPs for the particular type of morphologies is expected to be a competitive alternative to existing physical and chemical methods.

Key words: Pear Extract, Gold Nanoparticles, Stabilization, Green Chemistry, Circular Dichroism

INTRODUCTION

Engineered nanomaterials, including nanoparticles, nanotubes, and nano-wires, are at the leading edge of the rapidly developing field of nanotechnology. They are increasingly being used in a variety of commercial applications such as electronic, pharmaceutical, cosmetic, environmental, energy, and material uses [1,2]. Several methods have been regularly developed for the synthesis and surface functionalization of nanoparticles, particularly with chemical reagents having a toxic and aggressive nature, which includes several reducing agents, surface capping surfactants, and shape- and size-directing agents [3-5]. However, chemical methods have several negative impacts such as the hazardous nature of reagents, solvents, and the reducing environment, which could result in the adsorption and contamination of the final nano-product and generation of several risky by-products. Therefore, integration of green chemistry should be focused on during the synthesis and functionalization of nanomaterials, especially when nanomaterials are to be used in medical applications [6,7].

Biological building blocks are an extremely rich and useful resource for the synthesis of metal nanoparticles [8-10]. Most of the previous studies conducted for biological synthesis employed biomolecules such as proteins, amino acids, carbohydrates, and sugars; or, they employed either different types of microbial species or dissimilar plant resources (roots, leaves, flowers, bark powders, seeds, roots, and fruits) for the synthesis of metal nanoparticles [5,10-13]. It has been reported that the active species of the reaction mixture obtained from biological resources direct the shape and size of nanoparticles [14]. In addition, the reaction environment, process variables, and the effectiveness of the reductant also govern the size and shape [15-17]. There is tremendous scope for improvements in the synthesis of metal nanoparticles, such as the involvement of active species, viability of process, possibilities of size and shape control, stabilization of inorganic surfaces, and non-toxic nature of the final nano-product. Thus, there is a need to further explore green chemistry principles.

Herein, a simple, environmentally friendly, and self-sufficient biosynthetic approach was investigated for the preparation of GNPs with pear extract without using any external toxic or aggressive chemicals. The efforts were aimed at achieving size- and shape-controlled synthesis to investigate the importance of the reaction environment on the growth of nanoparticles in aqueous solution. Comprehensive characterization of obtained GNPs (including the average core size, morphology, purity, surface capping, crystal structure, and optical properties) was carried out by UV/Vis spectroscopy, transmission electron microscopy (TEM), X-ray diffraction (XRD), Fourier transform infrared spectroscopy (FT-IR), and circular dichroism (CD) spectral analysis.

MATERIALS AND METHODS

1. Materials

Chloroauric acid ($HAuCl_4$) was purchased from Sigma-Aldrich Korea. Fresh *Pyrus pyrifolia* (pear) fruits were obtained from the local marketplace. Pear species is native to China, Japan, and Korea. Pear is cultivated throughout East Asia, as well as in Australia, India, New Zealand, and other countries. The pear fruit differs in terms of size, shape, color, taste and storage qualities. The peel of the fresh pear was golden yellow and the white colored mesocarp was juicy. The major phytochemicals of pear fruits are carbohydrates, sugars, proteins, vitamins, amino acids and organic acids as reported by USDA National Nutrient Database [18]. The yellow pear extract was prepared as follows, in accordance with the typical preparation method. The peeled, white-colored watery flesh was crushed using a food processor, filtered through a mesh, and centrifuged twice at

†To whom correspondence should be addressed.
E-mail: daesung@knu.ac.kr

15,000 rpm for 20 min at 4 °C to remove any cell-free debris. The resulting supernatant was then passed through a 0.4-μm filter, and the final filtrate was employed to explore the reduction of gold precursor into the GNPs. The effects of biomass concentration and temperature on the synthesis of gold nanoparticles were investigated at constant pH 6.5.

2. Synthesis of Gold Nanoparticles and Nanoplates

Complete bioreduction was carried out to reduce Au(III) to Au(0) using pear extract to control the size and shape of the GNPs. The reduction rate of gold ions, surface plasmon resonance (SPR) properties, and the size and shape of the prepared GNPs were investigated under conditions of varying the pear extract concentration and temperature from 30 °C to 90 °C. Nine different variables were employed as a "single variable factor" at a time. In representative trials, a pre-incubated form of a 1-mM $HAuCl_4$ aqueous reaction mixture and the pear extract was set aside individually for 5 min under the selected temperature conditions to achieve thermal equilibrium. The reduction of the gold ions was started by adding increasing fractions of pear extract from 5, 15, and 45% (v/v) (denoted as F5, F15, and F45 respectively) at 30, 60, and 90 °C in triplicates. Optical and morphological properties from a particular reaction environment were representative in governing the SPR band and the morphologies of the obtained GNPs.

3. Characterization of Gold Nanoparticles and Nanoplates

The obtained GNPs were characterized in terms of the average core size, morphologies, physical properties (e.g., optical properties and crystal structure), and surface chemistry (capping) using the following techniques. The bioreduction and optical properties were studied by measuring the UV/Vis spectrum between 400 and 700 nm in a 10-mm-path-length quartz cuvette at 1-nm resolution (UV/Vis, Agilent Model-8453). TEM samples were prepared by drop casting on carbon-coated lacey films. The films were dried prior to the measurement of GNPs at an accelerating voltage of 30 kV using a CCD camera (Hitachi H-7600 AMT V600). Chemical properties of the GNPs were analyzed using energy-dispersive X-ray spectroscopy (EDS), which detects the fluorescent X-rays emitted from illuminated regions of the sample. Elemental identification was performed using energy dispersive X-ray analysis (EDS) attachment (F20 G2) operated at an accelerating voltage of 120 kV. Nanoparticle aqueous solutions were drop-cast onto a glass substrate to measure the XRD (Model D/Max-2500). Scanning was carried out in a 2θ region of 30-80°. The pattern was recorded using Cu-K_α radiation with a wavelength (λ) of 1.5406 Å at a tube voltage of 40 kV and tube current of 30 mA. FT-IR analysis was carried out after the removal of free biomolecules that was not adsorbed to the nanoparticles by repeated centrifugation (12,000 rpm for 30 min at 4 °C) and redispersion in water. Thereafter, the purified nanoparticle suspension was subjected to FT-IR analysis (Spectrum GX). The CD spectral analysis of dispersed GNPs in water was carried out to study peptide capping using a 10-mm quartz cuvette. After incubation for 4 min at 24 °C, CD spectra were collected from 250 nm to 190 nm using a spectrophotometer (Jasco, 810). The average of five scans was recorded at a scanning rate of 20 nm/min, using a time response of 8 s. The peptide capping on the surface of GNPs was confirmed by repeated scanning at different concentrations of the aqueous suspension.

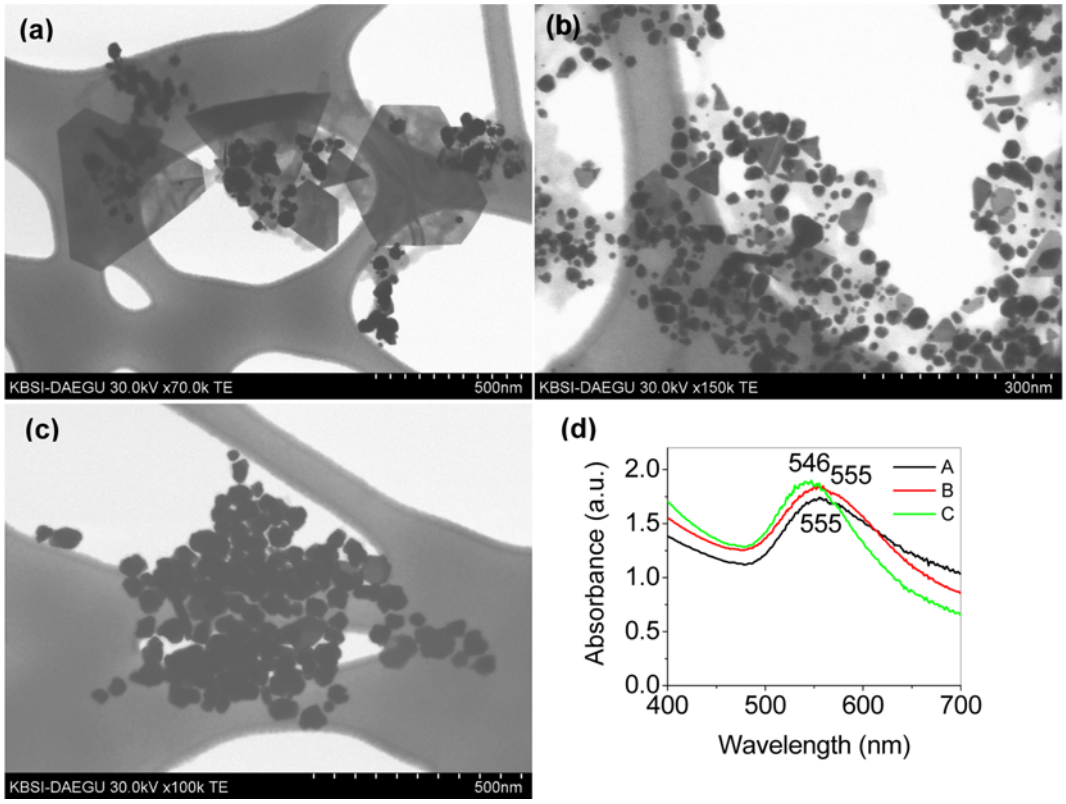

Fig. 1. Representative TEM images of GNPs synthesized at different pear extract concentrations: (a) F5, (b) F15, and (c) F45; (d), corresponding UV/Vis spectra of the GNPs ((a), (b), and (c)) at 30 °C.

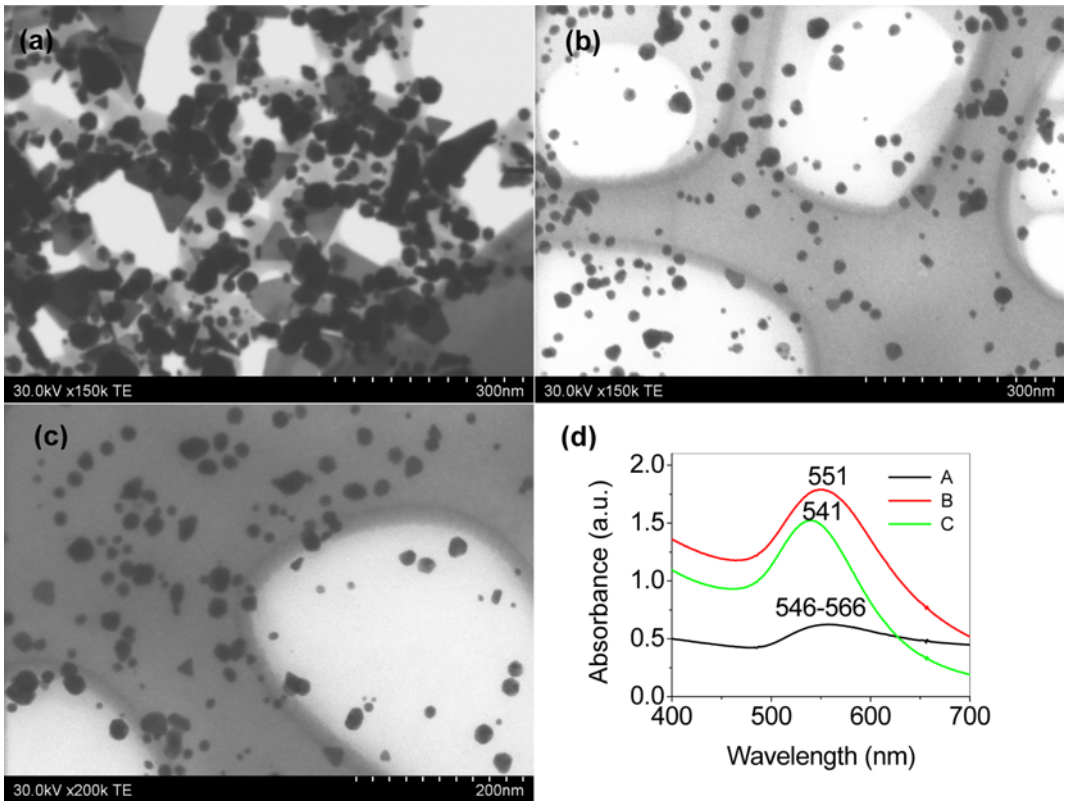

Fig. 2. Representative TEM images of GNPs synthesized at different pear extract concentrations: (a) F5, (b) F15, and (c) F45; (d), corresponding UV/Vis spectra of the GNPs ((a), (b), and (c)) at 60 °C.

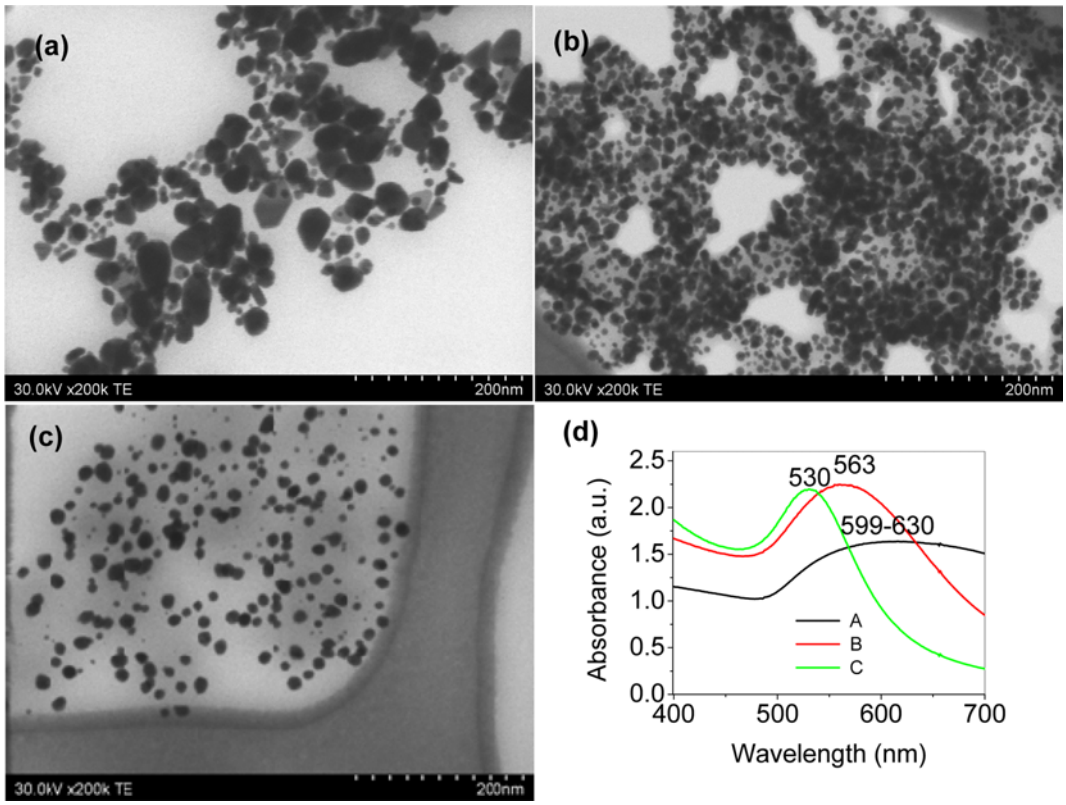

Fig. 3. Representative TEM images of GNPs synthesized at different pear extract concentrations: (a) F5, (b) F15, and (c) F45; (d), corresponding UV/Vis spectra of the GNPs ((a), (b), and (c)) at 90 °C.

RESULTS AND DISCUSSION

1. Optical Properties of Gold Nanoparticles and Nanoplates

Size- and shape-dependent synthesis of metal nanoparticles is a major challenge in the development of more facile and efficient methods. In the present study, efforts were aimed at monitoring the reduction kinetics, the growth of nanoparticles in aqueous solutions, and investigating the importance of reaction environment in the size- and shape-controlled synthesis. The pear-extract-based preparation of the GNPs was achieved by the simple mixing of an aqueous solution of $HAuCl_4$ (1 mM) in various reaction environments. The unusual color appearances ranging from blue, violet, and red were indications of the effects of the reaction environment. The optical properties, reaction kinetics, and conversion of gold ions into GNPs were monitored by UV/Vis spectroscopy. The formation of GNPs in all fractions was initially investigated for color change and their respective λ signal as presented in Table 1. In particular, the reaction variables were found to be constructive and extremely reproducible for guiding the shape and size of the GNPs (Figs. 1-3). The visible color is the effect of interaction of resonant light with GNPs, via excitation of surface plasmon by light scattering and absorption [17]. Pear extracts have the ability to reduce Au(III) to Au(0). The time required for the complete conversion of gold ions into GNPs under different reaction conditions was found to be critical (Table 1). The rapid reduction of gold ions was facilitated by increasing concentrations of the pear extract and increasing temperature (i.e., free energy).

An intermediate UV/Vis spectrum was recorded as a function of the reaction time. It was observed that the absorbance increased steadily and was finally stable at a particular level on the basis of reducing potential of reaction environment. We noticed a blue shift from 555 to 546, 546-566 to 541, and 599-630 to 530 nm with increasing pear extract concentrations at 30, 60, and 90 °C, respectively (Figs. 1(d), 2(d), and 3(d)). The largest gap of respective λ signals from 599-630 to 530 nm was found at 90 °C with increasing pear extract concentrations (F5 to F45% (v/v)). The obtained SPR peak with F45 at 60 and 90 °C showed a single absorption band throughout the reaction time at 541 and 530 nm, respectively, indicating consistency in particle size and shape from the beginning until the end of the reduction reaction of gold ions (Figs. 2(d) and 3(d)). In particular, with an increase in the concentration of the pear extract and reaction temperature, the SPR bands narrowed (Figs. 1(d), 2(d), and 3(d)). In the case of F5 at 30, 60, and 90 °C, the initially formed gold crystal nuclei could grow subsequently via edges; thus, it can be said that they followed an anisotropic growth pattern and formed plate-shaped nanostructures (Figs. 1, 2, and 3). The appearance of the broad band and transverse plasmon vibration with F5 at 60 and 90 °C could also be explained in terms of the plate-like and mixed morphologies (Figs. 2(d) and 3(d)) as reported earlier [17].

2. Characterization of Gold Nanoparticles and Nanoplates

Increasing the reductant concentration from 5 to 45% (v/v) and reaction temperature from 30 to 90 °C influenced the GNP morphologies from plate-like to spherical-shaped. The broad range of morphologies and size were evidenced for F5 (30, 60, and 90 °C) with several triangular, hexagonal, and polyhedral morphologies of gold nanoplates. With a decrease in the reductant concentration from 45 to 5% (v/v), the reaction completion time increased. Furthermore, with an increase in temperature from 30 to 90 °C, the reaction time and nanoparticle size decreased (Table 1, Figs. 1, 2, and 3). The pear-extract-concentration-dependent GNP sizes generated with F5, F15, and F45 at 30 °C are 20-400, 50±25, and 40±20 nm, respectively; those at 60 °C are 70±25, 20±9, and 20±6 nm, respectively; finally, the corresponding sizes at 90 °C are 40±20, 20±9, and 10±5 nm, respectively. (Table 1, Figs. 1, 2, and 3). Therefore, changing the pear extract concentrations and reaction temperature was an effective approach for determining the importance of reductant effectiveness in the nanoparticle growth process. The pear extract was accountable for the healthy capping of the GNPs obtained with F45 at both 60 and 90 °C. Thus, the colloidal solution was stable against agglomeration or aggregation as observed in a single narrow SPR peak and GNPs in TEM images (Figs. 2 and 3). Thus, F45 at both 60 and 90 °C was considered as being most favorable for the reduction of gold ions and stabilization of GNPs, which supports the formation of highly dispersed and identical spherical particles. Predominantly, nano-sized spherical gold particles exhibit only one SPR peak. However, broadening of the SPR band and aggregation with both F5 and F15 from 30 to 90 °C were caused by the combined effects of diverse GNP morphologies and unavailability of sufficient capping agents in colloidal solution. The tendency toward the aggregation and the wide-ranged size and shape is in agreement with the results of some previous studies [10-11,15]. GNPs with anisotropic nature and/or those prone to aggregation are responsible for the broadening of absorption peak from transverse and longitudinal SPR and this property depends on the shape and size of nanoparticles [19-21].

Obtained GNPs with F45 at 90 °C were subjected to detailed characterization (including capping, purity, and crystalline nature) by

Table 1. Characteristics of GNPs under different reaction conditions

Temperature (°C)	Reductant % (v/v)	Time	SPR (λ)	Morphology and size
30	5	12 hr	555	Spheres and plates (20-400 nm)
	15	9 hr	555	Spheres and plates (10-75 nm)
	45	6 hr	546	Asymmetrical NPs (40±20 nm)
60	5	300 min	546-566	Spheres and plates (10-100 nm)
	15	180 min	551	Spheres (20±9 nm)
	45	45 min	541	Spheres (20±6 nm)
90	5	90 min	599-630	Spheres and plates (10-60 nm)
	15	45 min	563	Spheres (20±9 nm)
	45	20 min	530	Spheres (10±5 nm)

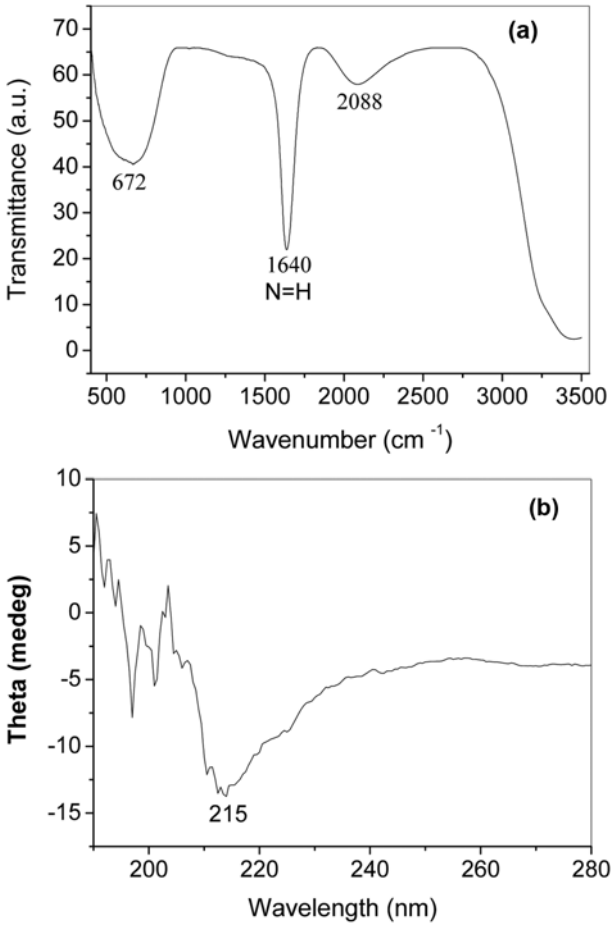

Fig. 4. (a) FT-IR spectrum of obtained GNPs with F45 at 90 °C. The spectrum shows the characteristic amide band of proteins. (b) CD spectrum of GNPs obtained with F45 at 90 °C. The spectrum shows the presence of capped proteins.

FTIR, CD, EDS, selected area (electron) diffraction (SAED), and XRD analysis. To investigate the capping of GNPs, purified suspensions of gold particles were analyzed by FT-IR and CD analyses. The FT-IR spectrum confirmed the expected occurrence of aldehydic C-H stretching (around 2,088 cm^{-1}) and a prominent peak at 1,640 cm^{-1}, indicating the capping of the GNPs by sugars, amino acids, and peptides (Fig. 4(a)). To confirm the existence and nature of the healthy capping of the GNPs by peptides originating from the pear extract, CD spectral analysis was carried out. The CD spectrum of the obtained GNPs with F45 at 90 °C showed a negative broad maximum at 215 nm, indicating a stable right-handed α-helix structure (Fig. 4(b)). These results of the CD and FT-IR analyses reveal that the sugars and peptides of the pear extract not only ensure the effective reduction of gold ions, but also successfully cap the newly formed GNPs, which could play a role in the protection of the GNP surface. The favorable organization and/or capping of biogenic GNPs by proteins and peptides is an example of biomimetic extracellular biomineralization. GNPs obtained from a soybean phytochemical mixture also exhibited the ability of being capped, thus enabling the gold nanoparticles to be shielded from aggregation [22].

Dark-field S-TEM images of GNPs obtained with F45 at 90 °C revealed electron-dense regions of GNPs (white) and the electron-lucent (black) as the background of carbon film (Fig. 5(a)). Single crystal selected area electron diffraction (SAED) patterns, obtained from collective GNPs, show crystalline nature (Fig. 5(c)).

This circular nature of SAED spots of GNPs (Fig. 5(b)) indicates a ring-like diffraction pattern; the particles were crystalline (Fig. 5(c)). EDS measurements of GNPs obtained with F45 at 90 °C revealed strong peaks corresponding to Au K- and L-edges (Fig. 6), representing the composition and purity of the gold phase. The peaks for copper and carbon were also found, but those originated from the carbon-coated copper grids used for TEM sample preparation and EDS analysis. A structural analysis of the GNPs obtained with F45 at 90 °C was performed by XRD. The angular positions of the Bragg peaks (Fig. 7) were preferentially oriented along the (111) plane, and a weak broad peak was observed as being oriented along the (200) plane. The observed "d-values" of the samples (from XRD patterns) correlate well with the standard "d-values" in the JCPDS data card 04-0784 for Au, which corroborates the for-

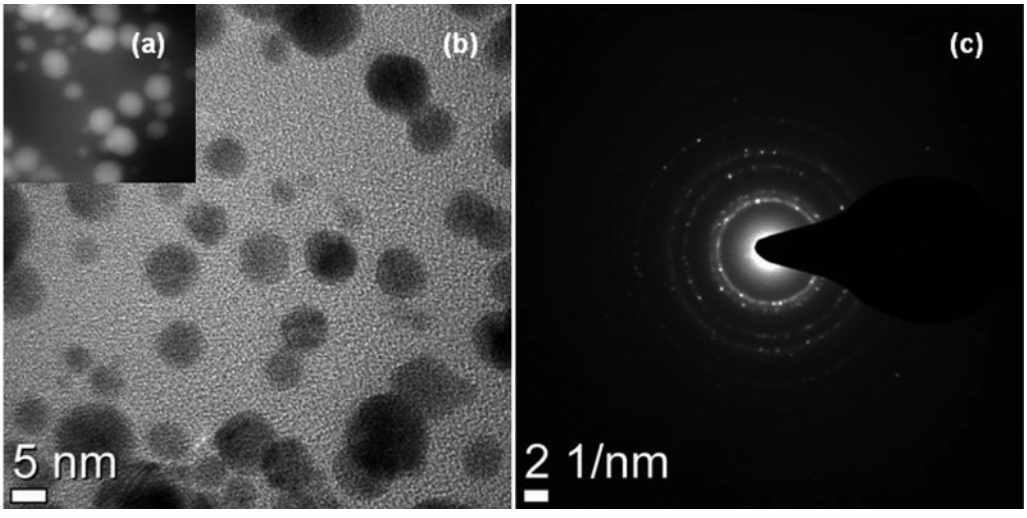

Fig. 5. (a) S-TEM micrographs of obtained GNPs with F45 at 90 °C, (b) representative TEM images, and (c) SAED pattern of corresponding GNPs.

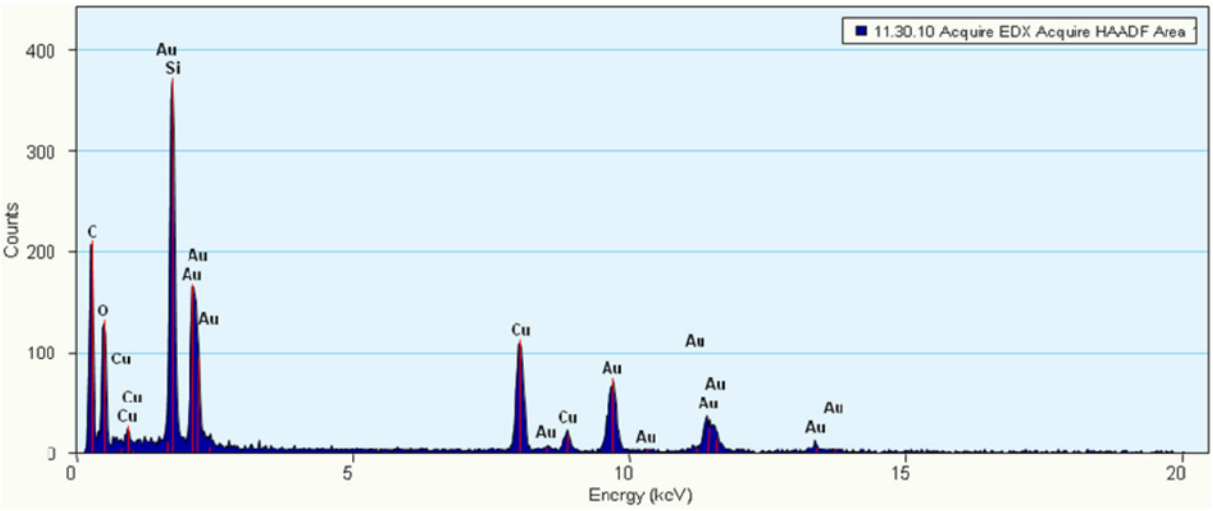

Fig. 6. EDS spectra of the obtained GNPs with F45 at 90 °C.

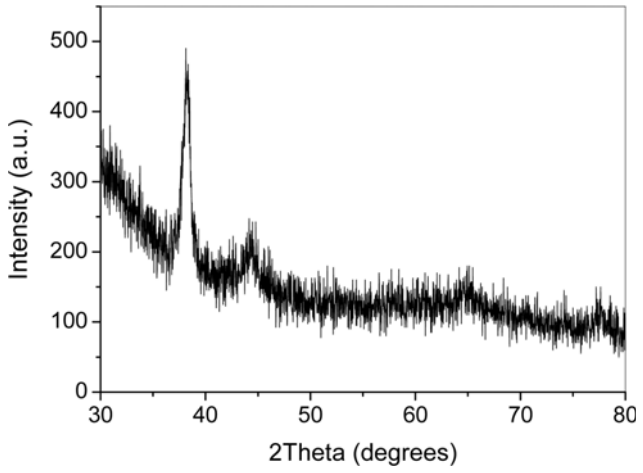

Fig. 7. XRD spectrum of the obtained GNPs with F45 at 90 °C.

mation of crystalline GNPs.

Bimolecular crystallization occurring on the plane of the nanoparticles could be a basis for the crystalline nature of GNPs. The formation of gold atoms Au(0) leads to their saturation or supersaturation; subsequently, gold atoms Au(0) initiate allocation to the existing nuclei and grow into GNPs via predesigned direction at nucleation phase. The optimal reduction potential permits the isotropic growth pattern, which plays a prominent role in rapid reduction of gold ions and formations of identical GNPs. Both anisotropy for the higher-order nanostructures (nanoplates) and isotropy for the spherical GNP could be practiced on the basis of appropriate reduction potentials. The deposition of Au atoms (crystal growth) occurs at particular higher surface energy faces with faster rate as compared to the rest of the surfaces, which is based on the reduction potential of reaction. The reduction potential provided by a particular reaction condition plays a key role in designing the faces at nucleation stage and they could prevent or allow a particular growth pattern. Thus, the bio-mimetic materialization could take advantages of pear extract-based biomolecules to engineer the surfaces of GNPs for biomolecular capping and surface-mediated growth. Therefore, the results of the present study will aid the tuning of morphology-based nanoparticles, exploration of biosynthesis mechanisms, and application of GNPs.

CONCLUSIONS

A controlled reduction of $HAuCl_4$ into GNPs was achieved using pear extract. The basic aspects of green chemistry were considered for the preparation of GNPs, which includes the use of an aqueous solvent and a safe, reducing, and stabilizing environment; therefore, the process is nonpolluting. The possibilities of growing GNPs to achieve both anisotropy for the higher-order nanostructures (nanoplates) and isotropy for the spherical nanoparticles were investigated on the basis of appropriate reaction conditions. Surface chemistry analysis of the GNPs revealed that peptides and/or proteins as key biomolecules of the pear extract played a significant role in Au(III) reduction, which subsequently resulted in healthy capping of GNPs. Green preparation of GNPs in risk-free aqueous media has been established for their safe and advanced applications in materials science, optoelectronic and biomedical technologies.

ACKNOWLEDGEMENT

This work was supported by the Basic Science Research Program through the National Research Foundation of Korea (NRF) and funded by the Ministry of Education, Science and Technology (MEST) (2011-0001115). This work was also partially supported by the second phase of the Brain Korea 21 Program in 2011 as well as by the Priority Research Centers Program through the NRF funded by MEST (2010-0028301). This work is also the outcome of a Manpower Development Program for Energy & Resources supported by the Ministry of Knowledge and Economy.

REFERENCES

1. R. J. Chen, S. Bangsaruntip, K. A. Drouvalakis, N. W. S. Kam, M. Shim, Y. Li, W. Kim, P. J. Utz and H. Dai, *Proc. Natl. Acad. Sci.*, **100**, 4984 (2003).

2. B. Nowack and T. D. Bucheli, *Environ. Pollut.*, **150**, 5 (2007).
3. S. Meltzer, R. Resch, B. E. Koel, M. E. Thompson, A. Madhukar, A. Requicha and P. Will, *Langmuir*, **17**, 1713 (2001).
4. A. Gole and C. J. Murphy, *Chem. Mater.*, **16**, 3633 (2004).
5. J. A. Dahl, B. L. S. Maddux and J. E. Hutchison, *Chem. Rev.*, **107**, 2228 (2007).
6. J. E. Hutchison, *ACS Nano*, **2**, 395 (2008).
7. H. Li, J. D. Carter and T. H. LaBean, *Mater. Today*, **12**, 24 (2009).
8. C. M. Niemeyer and B. Ceyhan, *Ange. Chem. Inter. Edi.*, **40**, 3685 (2001).
9. C. J. Tsai, J. Zheng, D. Zanuy, N. Haspel, H. Wolfson, C. Aleman and R. Nussinov, *Proteins*, **68**, 1 (2007).
10. V. Kumar and S. K. Yadav, *J. Chem. Technol. Biotechnol.*, **84**, 151 (2009).
11. P. Mohanpuria, N. K. Rana and S. K. Yadav, *J. Nanopart. Res.*, **10**, 507 (2008).
12. J. Huang, W. Wang, L. Lin, Q. Li, W. Lin, M. Li and S. Mann, *Chem. Asian J.*, **4**, 1050 (2009).
13. L. Castro, M. L. Blázquez, F. González, J. A. Muñoz and A. Ballester, *Chem. Eng. J.*, **164**, 92 (2010).
14. S. S. Shankar, A. Rai, B. Ankamwar, A. Singh, A. Ahmad and M. Sastry, *Nat. Mater.*, **3**, 482 (2004).
15. Y. N. Tan, J. Y. Lee and D. I. C. Wang, *J. Phys. Chem. C*, **112**, 5463 (2008).
16. J. Y. Song, H. K. Jang and B. S. Kim, *Process Biochem.*, **44**, 1133 (2009).
17. A. Tripathy, A. M. Raichur, N. Chandrasekaran, T. C. Prathna and A. Mukherjee, *J. Nanopart. Res.*, **12**, 237 (2010).
18. USDA National Nutrient Database for Standard Reference, Release 23. U.S. Department of Agriculture, Agricultural Research Service, Scientific Name: *Pyrus pyrifolia* (Pears, asian, raw) NDB No: 09340 (2010).
19. S. M. Nie and S. R. Emery, *Science*, **275**, 1102 (1997).
20. M. A. El-Sayed, *Accounts Chem. Res.*, **34**, 257 (2001).
21. L. M. Liz-Marzan, *Langmuir*, **22**, 32 (2006).
22. R. Shukla, S. K. Nune, N. Chanda, K. Katti, S. Mekapothula, R. R. Kulkarni, W. V. Welshons, R. Kannan and K. V. Katti, *Small*, **4**, 1425 (2008).